Monthly Notices
of the
ROYAL ASTRONOMICAL SOCIETY

MNRAS **472,** L115–L119 (2018)
Advance Access publication 2017 October 5

doi:10.1093/mnrasl/slx163

Classification of extremely metal-poor stars: absent region in A(C)–[Fe/H] plane and the role of dust cooling

Gen Chiaki,[1]★ Nozomu Tominaga[1] and Takaya Nozawa[2]

[1]*Department of Physics, Konan University, 8-9-1 Okamoto, Kobe 658-0072, Japan*
[2]*Division of Theoretical Astronomy, National Astronomical Observatory of Japan, Mitaka, Tokyo 181-8588, Japan*

Accepted 2017 October 2. Received 2017 September 8; in original form 2017 September 8

ABSTRACT

Extremely metal-poor (EMP) stars are the living fossils with records of chemical enrichment history at the early epoch of galaxy formation. By the recent large observation campaigns, statistical samples of EMP stars have been obtained. This motivates us to reconsider their classification and formation conditions. From the observed lower limits of carbon and iron abundances of $A_{\rm cr}({\rm C}) \sim 6$ and $[{\rm Fe/H}]_{\rm cr} \sim -5$ for C-enhanced EMP (CE-EMP) and C-normal EMP (CN-EMP) stars, we confirm that gas cooling by dust thermal emission is indispensable for the fragmentation of their parent clouds to form such low mass, i.e. long-lived stars, and that the dominant grain species are carbon and silicate, respectively. We constrain the grain radius $r_i^{\rm cool}$ of a species i and condensation efficiency f_{ij} of a key element j as $r_{\rm C}^{\rm cool}/f_{\rm C,C} = 10$ μm and $r_{\rm Sil}^{\rm cool}/f_{\rm Sil,Mg} = 0.1$ μm to reproduce $A_{\rm cr}$(C) and $[{\rm Fe/H}]_{\rm cr}$, which give a universal condition $10^{[{\rm C/H}]-2.30} + 10^{[{\rm Fe/H}]} > 10^{-5.07}$ for the formation of every EMP star. Instead of the conventional boundary $[{\rm C/Fe}] = 0.7$ between CE-EMP and CN-EMP stars, this condition suggests a physically meaningful boundary $[{\rm C/Fe}]_{\rm b} = 2.30$ above and below which carbon and silicate grains are dominant coolants, respectively.

Key words: stars: formation – stars: low-mass – stars: Population II – ISM: abundances – dust, extinction – galaxies: evolution.

1 INTRODUCTION

Long-lived stars with metallicities lower than our neighbourhood, so-called metal-poor (MP) stars, are discovered in our Galaxy and nearby dwarf galaxies. They are intensively studied as the clues to know the chemical evolution during the structure formation. This approach is called Galactic archaeology or near-field cosmology. MP stars are classified into carbon-enhanced MP (CEMP) and carbon-normal MP (CNMP) stars, divided at the boundary conventionally defined as $[{\rm C/Fe}] = 0.7$ (Beers & Christlieb 2005; Aoki et al. 2007).[1] CEMP stars are further divided into CEMP-no without the enhancement of neutron-capture elements, and CEMP-r or CEMP-s with r-process or s-process element enhancement, respectively (Beers & Christlieb 2005).

By recent large observational campaigns,[2] we can access the statistical samples of MP stars. Yoon et al. (2016) report that CEMP stars are apparently subdivided into three groups on the A(C)–[Fe/H] plane (Fig. 1). While CEMP Group I stars residing in $-3.7 < [{\rm Fe/H}] < -1.2$ and $7.0 < A({\rm C}) < 9.0$ are dominantly CEMP-s stars, Group II (with $-5.0 < [{\rm Fe/H}] < -2.5$ and $5.0 < A({\rm C}) < 7.0$) and Group III (with $[{\rm Fe/H}] < -3.5$ and $6.0 < A({\rm C}) < 7.5$) stars are mainly CEMP-no stars. Since almost all Group I stars show binary feature, they are considered to have acquired the gas rich with C and n-capture elements from their evolved companions (Suda et al. 2004). On the other hand, the physical explanation of distinction between Groups II and III stars has not been made so far.

MP stars with $[{\rm Fe/H}] < -3$ including CEMP Groups II and III stars are particularly called extremely metal-poor (EMP) stars. The lower limits of their elemental abundances indicate the existence of the critical metallicity above which their parent clouds become unstable to fragment into small gas clumps through efficient gas cooling by heavy elements so that low-mass stars which survive until the present day are likely to be formed (Bromm & Loeb 2003; Frebel et al. 2005). Recent theoretical studies have shown that cooling by dust thermal emission is crucial to form low-mass fragments with $\sim 0.1\,{\rm M}_\odot$ (Omukai 2000; Schneider et al. 2003).

Marassi et al. (2014) and Chiaki et al. (2015) predict that dust grains are important commonly for the formation of C-enhanced EMP (CE-EMP) and C-normal EMP (CN-EMP) stars. They show that the dominant grain species are carbon and silicate, respectively,

★ E-mail: chiaki@center.konan-u.ac.jp

[1] The ratio between abundances of elements j and k are expressed as $[j/k] = \log[y(j)/y(k)] - \log[y_\odot(j)/y_\odot(k)]$ and $A(j) = \log\epsilon(j) = 12 + \log y(j)$ for an element j, where $y(j)$ denotes the number fraction of j relative to hydrogen nuclei.

[2] e.g. the HK (Beers, Preston & Shectman 1985, 1992), Hamburg/ESO (Christlieb et al. 2001), SEGUE (Yanny et al. 2009), and LAMOST survey (Cui et al. 2012; Deng et al. 2012).

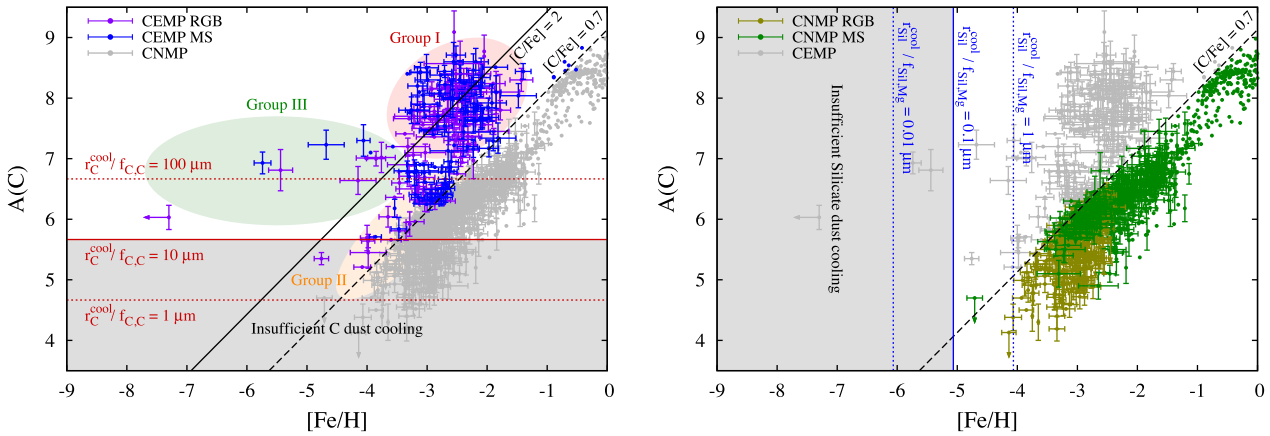

Figure 1. Carbon abundance A(C) as a function of metallicity [Fe/H] of observed CEMP stars (left-hand panel) and CNMP stars (right-hand panel) retrieved from SAGA data base (Suda et al. 2008, 2011, 2017; Yamada et al. 2013, http://sagadatabase.jp/). The dashed line represents [C/Fe] = 0.7 as the boundary between CEMP and CNMP stars (Beers & Christlieb 2005; Aoki et al. 2007). CEMP stars are further divided into three groups indicated by the ellipses in the left-hand panel (Yoon et al. 2016), and the solid line ([C/Fe] = 2.0) indicates the apparent boundary between Groups II and III. We show the critical carbon (equation 2) and iron (equation 4) abundances by red and blue lines, respectively, for various $r_C^{cool}/f_{C,C}$ and $r_{Sil}^{cool}/f_{Sil,Mg}$.

and estimate the critical C and Si abundances. However, they resort to theoretical models of grain formation because the properties of grains such as radius and condensation efficiency can not be directly measured. Further, their analyses are based on the conventional classification of EMP stars, and do not explain the difference between Groups II and III stars.

In this Letter, we reconsider the classification and formation conditions of EMP stars. From Fig. 1, we point out three interesting features: (1) no EMP stars have so far been observed in the region of A(C) < 6 and [Fe/H] < -5, (2) Groups III and II stars are distributed in the regions with high ([C/Fe] > 2) and moderate ([C/Fe] < 2) C-enhancement, respectively and (3) the distribution of Group II stars appears continuously connected with CN-EMP stars.

We derive grain properties of carbon and silicate from the feature (1), and then present a formation condition applicable to every EMP star. Comparing the contributions of carbon and silicate grains to gas cooling, we propose the physically motivated boundary between EMP stars whose formation could be derived mainly by carbon and silicate grains. This boundary can simultaneously explain the features (2) and (3). Throughout this Letter, we use the solar abundance of Asplund et al. (2009) as $A_\odot$(C) = 8.43, $A_\odot$(Mg) = 7.60 and $A_\odot$(Fe) = 7.50.

2 CRITICAL ELEMENTAL ABUNDANCES

The critical condition for cloud fragmentation can be described by the comparison of gas cooling owing to dust thermal emission with gas compressional heating (Schneider et al. 2012). With condensation efficiency f_{ij} of a key element j on to a grain species i and a characteristic grain radius r_i^{cool}, the fragmentation condition can be written using the number abundance $y(j)$ as

$$\sum_i \frac{3\mu_{ij} f_{ij} X_H}{4\varsigma_i r_i^{cool}} y(j) > 1.4 \times 10^{-3}\ \mathrm{cm^2\ g^{-1}}, \quad (1)$$

where μ_{ij} denotes the molecular weight of a monomer and ς_i is the bulk density of a grain (Chiaki et al. 2015).[3] This indicates that, once the key element and its abundance $y(j)$ are specified, we can put a constraint on r_i^{cool} and f_{ij} in a form of r_i^{cool}/f_{ij}, which we hereafter call the effective grain radius.

2.1 Critical C abundance and property of carbon grains

We first derive the effective radius $r_C^{cool}/f_{C,C}$ for carbon grains. For carbon grains, the key element is carbon, and $\mu_{C,C} = 12$ and $\varsigma_C = 2.23\ \mathrm{g\,cm^{-3}}$. Then, from equation (1), we can obtain the critical carbon abundance above which gas cooling by carbon grains exceeds gas compressional heating as

$$A_{cr}(C) = 5.67 + \log\left(\frac{r_C^{cool}/f_{C,C}}{10\ \mu m}\right). \quad (2)$$

The horizontal red lines in the left-hand panel of Fig. 1 show the critical carbon abundances for $r_C^{cool}/f_{C,C} = 1$, 10 and 100 μm from bottom to top. CEMP Group III stars are distributed in a range of A(C) > 6.0 over a wide range of [Fe/H] ($-7 \lesssim$ [Fe/H] $\lesssim -4$). Hence, $A_{cr}(C) = 6$ can be taken as the lower limit of C abundances for CEMP Group III stars. Then, the effective grain radius is estimated to be $r_C^{cool}/f_{C,C} = 21.6$ μm. Taking the statistical uncertainties into consideration, we here adopt $r_C^{cool}/f_{C,C} = 10$ μm. Below the horizontal line corresponding to $r_C^{cool}/f_{C,C} = 10$ μm (shaded region in Fig. 1), carbon dust cooling is inefficient to induce cloud fragmentation, and long-lived low-mass stars are unlikely to form. Some of CEMP Group II stars have lower carbon abundances than $A_{cr}(C) = 6.0$, which is discussed in the subsequent sections.

2.2 Critical Fe abundance and property of silicate grains

Next, we constrain the property of the other major grain species, silicate. For silicates, we consider enstatite ($MgSiO_3$) with its key element being Mg, and $\mu_{MgSiO_3,Mg} = 100$ and $\varsigma_{MgSiO_3} = 3.21\ \mathrm{g\ cm^{-3}}$.

[3] We here consider spherical grains. The radius r_i^{cool} is defined as $\langle r^3\rangle_i/\langle r^2\rangle_i$ characterizing the efficiency of gas cooling, where $\langle x\rangle_i = \int x\varphi_i(r)\mathrm{d}r$ is the average of a physical quantity x weighted by the size distribution $\varphi_i(r)$ of a grain species i. Equation (1) is given at the gas density $n_H = 10^{14}\ \mathrm{cm^{-3}}$ and temperature $T = 1000$ K, where dust cooling is dominant over gas compressional heating in clouds with [Fe/H] ~ -5 (Schneider et al. 2012). X_H is the mass fraction of hydrogen nuclei and $X_H = 0.75$ throughout this Letter.

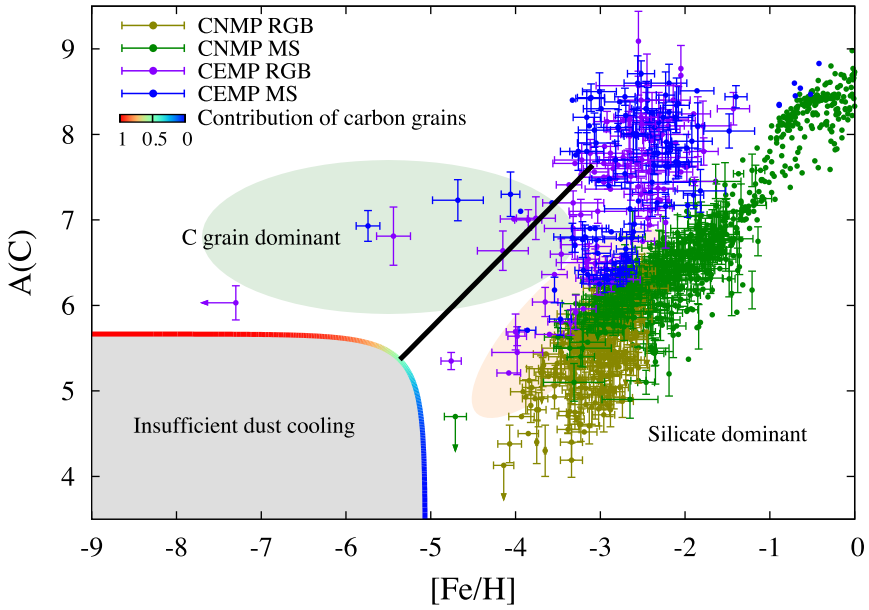

Figure 2. Carbon abundance A(C) as a function of [Fe/H] of Galactic halo MP stars ever observed. The formation of these long-lived, low-mass stars would be restricted by C and Fe abundances above which gas cooling by carbon and silicate grains exceeds gas compressional heating (equation 5) indicated by the curve coloured from blue to red with increasing fraction of the carbon grain cooling efficiency. The black line shows the boundary $[\mathrm{C/Fe}]_\mathrm{b} = 2.30$ (equation 6) above and below which carbon and silicate grains are dominant coolants for the formation of EMP stars, respectively.

The result is unchanged for forsterite (Mg_2SiO_4), whose key element is Si. From equation (1), we can calculate the critical condition where gas cooling by silicate grains overcomes the compressional gas heating as

$$[\mathrm{Mg/H}]_\mathrm{cr} = -4.70 + \log\left(\frac{r_\mathrm{Sil}^\mathrm{cool}/f_\mathrm{Sil,Mg}}{0.1\ \mu\mathrm{m}}\right). \quad (3)$$

We convert this critical Mg abundance to the critical Fe abundance, using the average abundance ratio [Mg/Fe] = 0.368 for stars with [Fe/H] < -1 (from SAGA data base), as

$$[\mathrm{Fe/H}]_\mathrm{cr} = -5.07 + \log\left(\frac{r_\mathrm{Sil}^\mathrm{cool}/f_\mathrm{Sil,Mg}}{0.1\ \mu\mathrm{m}}\right). \quad (4)$$

The vertical blue lines in the right-hand panel of Fig. 1 indicate the critical Fe abundances for $r_\mathrm{Sil}^\mathrm{cool}/f_\mathrm{Sil,Mg} = 0.01$, 0.1 and 1 μm from left to right. To realize the critical abundance $[\mathrm{Fe/H}]_\mathrm{cr} = -5.0$ suggested by the distribution of CN-EMP stars, the effective grain radius $r_\mathrm{Sil}^\mathrm{cool}/f_\mathrm{Sil,Mg} = 0.081$ μm is required. We set the fiducial value of the effective grain radius as $r_\mathrm{Sil}^\mathrm{cool}/f_\mathrm{Sil,Mg} = 0.1$ μm, which is smaller than that of carbon grains by two orders of magnitude.

2.3 Combined criterion for CE-EMP and CN-EMP star formation

In the previous sections, we have considered separately the contributions of carbon and silicate grains to gas cooling, and derived their effective grain radii. In reality, both the grain species can contribute simultaneously to gas cooling in collapsing clouds. In this case, equation (1) is reduced to

$$\frac{3.03}{r_\mathrm{C}^\mathrm{cool}/f_\mathrm{C,C}}y(\mathrm{C}) + \frac{17.5}{r_\mathrm{Sil}^\mathrm{cool}/f_\mathrm{Sil,Mg}}y(\mathrm{Mg}) > 1.4\times10^{-3}.$$

Using $r_\mathrm{C}^\mathrm{cool}/f_\mathrm{C,C} = 10$ μm and $r_\mathrm{Sil}^\mathrm{cool}/f_\mathrm{Sil,Mg} = 0.1$ μm derived in the previous sections gives

$$10^{[\mathrm{C/H}]-2.30} + 10^{[\mathrm{Fe/H}]} > 10^{-5.07}. \quad (5)$$

The critical condition is shown by the coloured curve in Fig. 2. The shaded region below the curve can successfully explain the region where no stars have been observed so far. Also, the figure suggests that the distribution of CEMP Group II stars shows the lower limit of Fe abundance at [Fe/H] $= -5$ as that of CN-EMP stars.

2.4 Boundary between CE-EMP and CN-EMP stars

Equating the first and second terms in the left-hand side of equation (5), we can define the transition line on which the contributions of carbon and silicate grains to gas cooling are equal as

$$[\mathrm{C/Fe}]_\mathrm{b} = 2.30. \quad (6)$$

This condition is indicated by the black line in Fig. 2 above which gas cooling by carbon grain is dominant over that by silicates. The boundary gives the physical explanation of the distinction between CEMP Group III and Group II stars.

3 MODEL CALCULATIONS OF GRAIN PROPERTIES IN POP III SN EJECTA

We have shown that the effective grain radius of carbon must be larger than that of silicate by two orders of magnitude to reproduce the observed distributions of EMP stars. In this section, we show this difference in grain radius with a dust formation model. In the early Universe, dust grains are mainly supplied by supernovae (SNe) arising from first-generation metal-free (Pop III) stars (Todini & Ferrara 2001; Nozawa et al. 2003). While the elemental abundances of CE-EMP stars are well reproduced by faint core-collapse SNe (FSNe) with C enhancement due to large fallback of Fe peak elements, those of CN-EMP stars are reproduced by energetic core-collapse SNe (CCSNe) or hypernovae (HNe) (Umeda & Nomoto 2003; Limongi & Chieffi 2012;

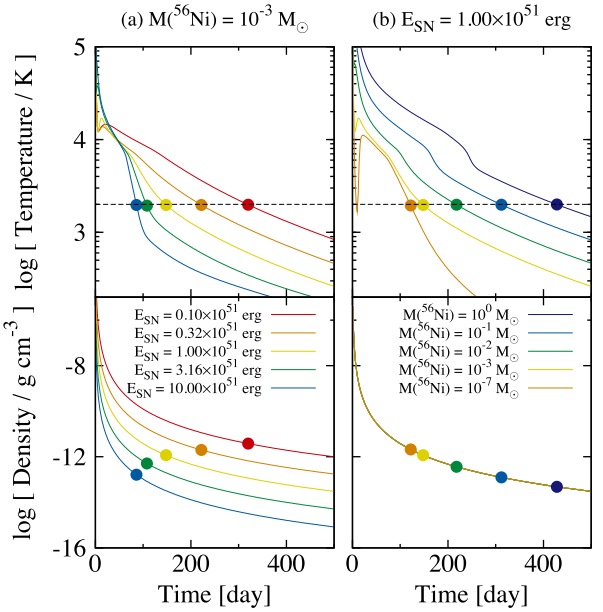

Figure 3. Time evolutions of gas temperature and density (a) with a fixed ^{56}Ni mass of $M(^{56}\mathrm{Ni}) = 10^{-3}\,\mathrm{M}_\odot$ and (b) with a fixed explosion energy of $E_{\rm SN} = 1 \times 10^{51}$ erg at the mass coordinate where the largest carbon grains are formed. The circles are plotted at the onset time of carbon grain formation when T becomes below the condensation temperature (2000 K) indicated by the black dashed line.

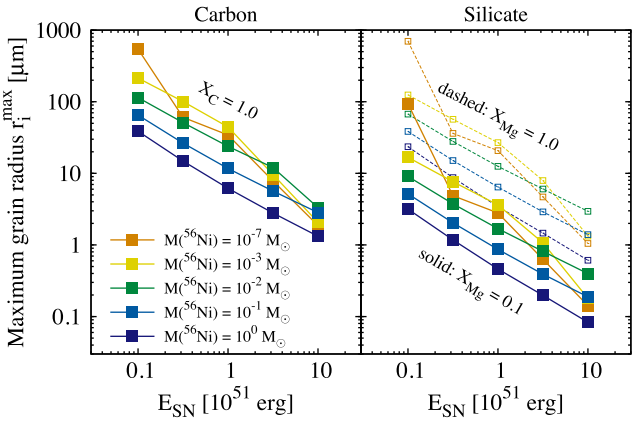

Figure 4. Maximum grain radius $r_i^{\rm max}$ of carbon (left) and silicate (right) grains as a function of explosion energy $E_{\rm SN}$ with various ^{56}Ni masses. For silicate grains, dashed and solid curves show the results with mass fraction $X_{\rm Mg}$ of the key element Mg of 1.0 and 0.1, respectively.

Ishigaki et al. 2014; Marassi et al. 2014; Tominaga, Iwamoto & Nomoto 2014).

To estimate the properties of newly formed dust, we follow the temporal evolution of temperature T and density ρ of expanding SN ejecta with radiative transfer calculations including energy deposition from radioactive decay of ^{56}Ni (Iwamoto et al. 2000). Applying the approximation formulae of Nozawa & Kozasa (2013), the average grain radius $r_i^{\rm ave}(M_{\rm R})$ and condensation efficiency $f_{ij}^{\rm ave}(M_{\rm R})$ are calculated at each mass coordinate $M_{\rm R}$ from the concentration $c_j^{\rm on} = X_j\rho/m_j$ of a key element j and the cooling time-scale $\tau_i^{\rm cool}$ at the onset time $t_i^{\rm on}$ of dust formation when T declines down to the condensation temperature (2000 K and 1500 K for carbon and silicate grains, respectively). A dominant fraction of grains will be formed at the mass coordinate $M_R^{\rm max}$, where $r_i^{\rm ave}$ becomes largest because $c_i^{\rm on}$ marks maximum there. We thus take $r_i^{\rm max} = r_i^{\rm ave}(M_R^{\rm max})$ as the fiducial value of the grain radius. At $M_R^{\rm max}$, $f_{ij}^{\rm ave}$ turns to be $\sim$1. We take a progenitor model of the SN which reproduces the chemical composition of HE0557 $-$ 4840 with an intermediate C-enhancement [C/Fe] = 1.68 (Ishigaki et al. 2014). The mass-cut is $M_{\rm cut} = 5.65\,\mathrm{M}_\odot$ and progenitor mass is $M_{\rm pr} = 25\,\mathrm{M}_\odot$. The masses of C and Mg atoms are $m_{\rm C} = 12m_{\rm H}$ and $m_{\rm Mg} = 24m_{\rm H}$, where $m_{\rm H}$ is the mass of a hydrogen nucleus.

We first see the results for carbon grains. Since carbon grains are formed mainly in the layer rich with C, we set $X_{\rm C} = 1.0$. Fig. 3 shows the temporal evolutions of gas temperature and density. With a fixed ^{56}Ni mass of $M(^{56}\mathrm{Ni}) = 1 \times 10^{-3}\,\mathrm{M}_\odot$, temperature and density for higher explosion energy $E_{\rm SN}$ decline more rapidly due to the higher expansion rate, and the time $t_{\rm C}^{\rm on}$ (indicated by circles) becomes earlier. With a fixed $E_{\rm SN} = 1 \times 10^{51}$ erg, temperature keeps higher, and $t_{\rm C}^{\rm on}$ becomes later for larger $M(^{56}\mathrm{Ni})$. Fig. 4 shows the grain radius $r_i^{\rm max}$ as a function of $E_{\rm SN}$ with various $M(^{56}\mathrm{Ni})$. For each $M(^{56}\mathrm{Ni})$, the grain radius is smaller for higher $E_{\rm SN}$ because the gas density is smaller at $t_{\rm C}^{\rm on}$ by more rapid expansion. For $M(^{56}\mathrm{Ni}) < 0.01\,\mathrm{M}_\odot$, $r_i^{\rm max}$ declines rapidly with $E_{\rm SN} \gtrsim 1 \times 10^{51}$ erg because $t_i^{\rm on}$ is coincident with the finishing time of the plateau phase when the ejecta becomes optically thin and the temperature decline suddenly. With shorter cooling time-scale, the larger number of grain seeds form, i.e, the radius of each grain becomes smaller.

With the same mass fraction $X_{\rm C} = X_{\rm Mg} = 1.0$, $r_i^{\rm max}$ for carbon and silicate grains are similar for each $E_{\rm SN}$ and $M(^{56}\mathrm{Ni})$. However, in the formation region of silicate grains, Mg is dominated by O, and we set the fiducial value as $X_{\rm Mg} = 0.1$, following nucleosynthesis calculations (Tominaga et al. 2014). With $X_{\rm Mg} = 0.1$, the $r_{\rm Sil}^{\rm max}$ decreases by an order of magnitude for each $E_{\rm SN}$ and $M(^{56}\mathrm{Ni})$.

To reproduce the elemental abundance of the most iron-poor CE-EMP stars such as SMSS J0313 $-$ 6708 (Keller et al. 2014), $E_{\rm SN} \sim 10^{51}$ erg and $M(^{56}\mathrm{Ni}) \lesssim 10^{-3}\,\mathrm{M}_\odot$ are favoured (Marassi et al. 2014; Ishigaki et al. 2014). In our calculations, we estimate $r_{\rm C}^{\rm max} = 34.3$ μm with $E_{\rm SN} = 1.0 \times 10^{51}$ erg and $M(^{56}\mathrm{Ni}) = 1 \times 10^{-7}\,\mathrm{M}_\odot$. The abundance ratio of the most metal-poor star SDSS J1029 + 1729 (Caffau et al. 2011) is reproduced by HN models with $E_{\rm SN} \sim 10^{52}$ erg and $M(^{56}\mathrm{Ni}) \sim 0.1\,\mathrm{M}_\odot$ (Tominaga et al. 2014). We predict $r_{\rm Sil}^{\rm max} = 0.188$ μm with $E_{\rm SN} = 1.0 \times 10^{52}$ erg, $M(^{56}\mathrm{Ni}) = 0.1\,\mathrm{M}_\odot$, and $X_{\rm Mg} = 0.1$. These values are consistent with $r_{\rm C}^{\rm cool}/f_{\rm C,C} = 10$ μm and $r_{\rm Sil}^{\rm cool}/f_{\rm Sil,Mg} = 0.1$ μm.

4 DISCUSSION

The observed lower limits of C and Fe abundances of CE-EMP and CN-EMP stars indicate that these stars form through the fragmentation of their parent clouds by gas cooling owing to thermal emission of two major grain species, carbon and silicate, respectively. We first derive the grain radius and condensation efficiency as $r_{\rm C}^{\rm cool}/f_{\rm C,C} = 10$ μm and $r_{\rm Sil}^{\rm cool}/f_{\rm Sil,Mg} = 0.1$ μm from the lower limits of C and Fe abundances, respectively. The tendency that carbon grains are larger than silicates is qualitatively explained by our simple analyses of dust formation. Carbon grains grow more efficiently than silicate because the gas density remains higher at the time when temperature declines to the condensation temperature with the smaller $E_{\rm SN}$ and $M(^{56}\mathrm{Ni})$ favoured for CE-EMP stars, and because the mass fraction of C is higher than that of Mg in the dust formation region.

We can derive the critical condition for EMP star formation as equation (5), which can well reproduce the region where no stars have so far been observed as indicated by the shaded region in

Fig. 2. Then, we find that the dominant coolant switches from carbon to silicate from above to below the boundary $[C/Fe]_b = 2.30$, which gives the physically motivated classification of CE-EMP and CN-EMP stars. This simultaneously explain the discrimination of CEMP Group II and Group III stars (Yoon et al. 2016). Opposite to Group III stars, the dominant coolant for the formation of CEMP Group II stars is silicate grains as CN-EMP stars. Interestingly, the distribution of Group II stars is continuous with that of CN-EMP stars as indicated by Fig. 2.

Our estimation of the effective grain radii is based on the observed elemental abundances of EMP stars. Our model presented in Section 3 predicts the larger values $r_C^{cool}/f_{C,C} = 34.3$ μm and $r_{Sil}^{cool}/f_{Sil,Mg} = 0.188$ μm for the fiducial cases. Although we here take the maximum grain radius at the corresponding mass coordinate M_R^{max}, the mass fraction of smaller grains formed in other mass coordinates can non-negligible, and the average radius of grains will be smaller. Marassi et al. (2015) predict the smaller grain radii of $r_C^{cool}/f_{C,C} \lesssim 0.1$ μm by their grain formation models in FSN ejecta. It is still possible that stars with lower elemental abundances, which is permitted by smaller effective grain radii, are discovered by future observations. In the current state, although the number of samples in the Galactic halo is large ($\sim 10^6$ stars), statistics of EMP stars with $[Fe/H] < -3$ is still small (Hartwig et al. 2015). As the number of EMP stars increases by future observations, the accuracy of the estimation of grain property and the boundary between CE-EMP and CN-EMP stars presented in this Letter will get improved.

ACKNOWLEDGEMENTS

We thank the referee for the positive comments and suggestions. GC is supported by Research Fellowships of the Japan Society for the Promotion of Science (JSPS) for Young Scientists. This work is supported in part by the Grants-in-Aid for Young Scientists (S: 23224004) and for General Scientists (A: 16H02168, C: 26400223) by JSPS.

REFERENCES

Aoki W., Beers T. C., Christlieb N., Norris J. E., Ryan S. G., Tsangarides S., 2007, ApJ, 655, 492
Asplund M., Grevesse N., Sauval A. J., Scott P., 2009, ARA&A, 47, 481
Beers T. C., Christlieb N., 2005, ARA&A, 43, 531
Beers T. C., Preston G. W., Shectman S. A., 1985, AJ, 90, 2089
Beers T. C., Preston G. W., Shectman S. A., 1992, AJ, 103, 1987
Bromm V., Loeb A., 2003, Nat, 425, 812
Caffau E. et al., 2011, Nature, 477, 67
Chiaki G., Marassi S., Nozawa T., Yoshida N., Schneider R., Omukai K., Limongi M., Chieffi A., 2015, MNRAS, 446, 2659
Christlieb N., Wisotzki L., Reimers D., 2001, A&A, 366, 898
Cui X. -Q. et al., 2012, Res. Astron. Astrophys., 12, 1197
Deng L. -C. et al., 2012, Res. Astron. Astrophys., 12, 735
Frebel A. et al., 2005, Nature, 434, 871
Hartwig T., Bromm V., Klessen R. S., Glover S. C. O., 2015, MNRAS, 447, 3892
Ishigaki M. N., Tominaga N., Kobayashi C., Nomoto K., 2014, ApJ, 792, L32
Iwamoto K. et al., 2000, ApJ, 534, 660
Keller S. C. et al., 2014, Nature, 506, 463
Limongi M., Chieffi A., 2012, ApJS, 199, 38
Marassi S., Chiaki G., Schneider R., Limongi M., Omukai K., Nozawa T., Chieffi A., Yoshida N., 2014, ApJ, 794, 100
Marassi S., Schneider R., Limongi M., Chieffi A., Bocchio M., Bianchi S., 2015, MNRAS, 454, 4250
Nozawa T., Kozasa T., 2013, ApJ, 776, 24
Nozawa T., Kozasa T., Umeda H., Maeda K., Nomoto K., 2003, ApJ, 598, 785
Nozawa T., Kozasa T., Habe A., Dwek E., Umeda H., Tominaga N., Maeda K., Nomoto K., 2007, ApJ, 666,955
Omukai K., 2000, ApJ, 534, 809
Schneider R., Ferrara A., Salvaterra R., Omukai K., Bromm V., 2003, Nature, 422, 869
Schneider R., Omukai K., Bianchi S., Valiante R., 2012, MNRAS, 419, 1566
Suda T., Aikawa M., Machida M. N., Fujimoto M. Y., Iben I., Jr, 2004, ApJ, 611, 476
Suda T. et al., 2008, PASJ, 60, 1159
Suda T., Yamada S., Katsuta Y., Komiya Y., Ishizuka C., Aoki W., Fujimoto M. Y., 2011, MNRAS, 412, 843
Suda T., Hidaka J., Aoki W., 2017, PASJ, 69, 76
Todini P., Ferrara A., 2001, MNRAS, 325, 726
Tominaga N., Iwamoto N., Nomoto K., 2014, ApJ, 785, 98
Umeda H., Nomoto K., 2003, Nature, 422, 871
Yamada S., Suda T., Komiya Y., Aoki W., Fujimoto M. Y., 2013, MNRAS, 436, 1362
Yanny B. et al., 2009, AJ, 137, 4377
Yoon J. et al., 2016, AJ, 833, 17

This paper has been typeset from a TEX/LATEX file prepared by the author.